Metallophysics and Advanced Technologies
Металофіз. новітні технол.
Metallofiz. Noveishie Tekhnol.
2019, vol. 41, No. 4, pp. 445–459
https://doi.org/10.15407/mfint.41.04.0445
Reprints available directly from the publisher

METALLIC SURFACES AND FILMS

PACS numbers: 64.70.dj, 68.35.bd, 68.35.Dv, 68.55.A-, 68.55.J-, 68.60.Dv, 81.16.-c

Formation of Island Structures During Melting Process of Tin Films on Amorphous Carbon Substrate

S. V. Dukarov, S. I. Petrushenko, V. M. Sukhov, and I. G. Churilov

V. N. Karazin Kharkiv National University,
4 Svobody Sqr.,
UA-61022 Kharkiv, Ukraine

The results of research devoted to formation of ordered arrays of particles during melting process of tin films on amorphous carbon substrate are given in the present work. Using scanning electron microscopy the histograms of particle size distribution are constructed for films of different mass thickness. The size dependences of the most probable radius of particles, which are formed during the melting process, and the half-width values of the corresponding histograms are obtained as well. The excess energy, which provides a decomposition of the initially continuous film into separate islands, is estimated and its size dependence is built. As shown, the melting process of films, which are condensed in island structures, provides larger filling coefficients in comparison with the melting process of initially continuous films.

Key words: annealing of films, thermal decomposition, histogram and half-width of distribution, excess energy.

В роботі представлено результати досліджень процесів формування впорядкованих масивів частинок при плавленні плівок олова на аморфній вуглецевій підкладці. Для плівок різної масової товщини за допомогою растрових електронно-мікроскопічних досліджень побудовано гістограми розподілу частинок за розмірами. Отримано розмірні залежності найбільш ймовірного радіуса частинок, що утворюються при плавленні, і півширини відповідних гістограм. Оцінено надлишкову енергію, що забезпечує розпад первісно суцільної плівки на окремі острівці, і побудовано її розмірну залежність. Показано, що плавлення плівок, конденсованих в

Corresponding author: Sergii Ivanovych Petrushenko
E-mail: petrushenko@univer.kharkov.ua

Citation: S. V. Dukarov, S. I. Petrushenko, V. M. Sukhov, and I. G. Churilov, Formation of Island Structures during Melting Process of Tin Films on Amorphous Carbon Substrate, *Metallofiz. Noveishie Tekhnol.*, **41**, No. 4: 445–459 (2019), DOI:10.15407/mfint.41.04.0445.

острівцеві структури, забезпечує більші коефіцієнти заповнення в порівнянні з плавленням суцільних плівок.

Ключові слова: відпал плівок, термічне диспергування, гістограма та напівширина розподілу, надлишкова енергія.

В работе представлены результаты исследования процессов формирования упорядоченных массивов частиц при плавлении плёнок олова на аморфной углеродной подложке. Для плёнок различной массовой толщины при помощи растровых электронно-микроскопических исследований построены гистограммы распределения частиц по размерам. Получены размерные зависимости наиболее вероятного радиуса частиц, образующихся при плавлении, и полуширины соответствующих гистограмм. Оценена избыточная энергия, обеспечивающая распад изначально сплошной плёнки на отдельные островки, и построена её размерная зависимость. Показано, что плавление плёнок, конденсированных в островковые структуры, обеспечивает большие коэффициенты заполнения по сравнению с плавлением изначально сплошных плёнок.

Ключевые слова: отжиг плёнок, термический распад, гистограмма и полуширина распределения, избыточная энергия.

(Received April 3, 2018)

1. INTRODUCTION

It is well known that the structure of thin films determines many technologically important properties of such systems [1–3]. In such a way, knowledge of the objective laws of the evolution of thin-film structures under the temperature impact is important for solving both general scientific and application tasks [4–6]. That is why the study of thermal dispersion of films makes it possible to obtain the unique information about the energy balance of low-dimensional structures. This is due to the fact that the driving force of film's decomposition is usually presented by the excess energy of the initially continuous film, which is connected with mechanical stresses and a branched chain of grain boundaries. On the other hand, the processes of dispersion of initially continuous films are of independent applied interest. Due to such processes, it is possible to form ordered arrays of particles, which in their turn have a wide potential for the practical use. Such structures are considered as active elements of photocatalytic generators, various sensors, light-emitting devices, elements of constant and operative memory, *etc*. [1, 7–9].

Vacuum methods of obtaining highly disperse arrays have a number of advantages of chemical technologies [10–12] which are widely used now. Thus, the condensation of samples and their dispersion under high vacuum conditions makes it almost completely possible to dispose

of uncontrolled impurities that have a primary influence on structures with a high surface fraction. In addition, a possibility to separate physically the particles on a substrate, allows potentially to working out nanoarrays, which do not require a stabilizer to prevent the coalescence of structures that are obtained by chemical methods [13–15].

The majority of practical applications, which are focused on using the arrays of nanoparticles, require the creation of structures with the narrowest possible size distribution. At the same time, in many cases, the particle size distribution in films, which were subjected to the thermal dispersion is broad and contains more than one maximum. Thus, for example, as it was determined in the work [16], the thermal annealing of palladium and platinum films on the oxide materials (at the temperature below the melting point) leads to decomposition of initially continuous films into separate islands.

An increase in both temperature and annealing time leads to an intensification of the dispersion processes, a decrease of the coverage of the substrate by the film and a change in the shape of particles, which become more rounded. The similar results were obtained in works [17, 18], in which authors explored the dispersion of single-component copper films and the decomposition of copper films stimulated by a small amount of liquid Pb. According to [18, 19] during the annealing of films of fusible metals near the melting temperature for a few minutes after heating, partial dispersion of films and the appearance of structures, which consist from irregularly shaped islands, occurs.

We note that particles of almost spherical shape arise in a regular manner during the melting process of films on poorly wetted surfaces. In this way, the results of works [20–22] indicate that during the melting process of films of fusible metals on oxide or amorphous carbon substrates, the formation of particles of practically spherical shape happens. The average size of such particles is primarily determined by the thickness of the original film.

The given work is devoted to study of morphology of island structures, which are formed during the melting process of continuous tin films on amorphous carbon substrate.

2. EXPERIMENTAL

Samples for the study were condensed in a vacuum of 10^{-6} Torr produced by oil-free pumping means. Tin was deposited from wolfram boats heated by direct passing of electric current, and the carbon condensed from a voltaic arc ignited between two graphite rods. Samples were deposited on fresh cleavages of KCl single crystals, which were fixed in a substrate holder—a copper massive heating block.

Structurally, the heating block was made in the form of a rectangular parallelepiped with dimensions of $150\times30\times10$ mm^3, along the long

side of which a number of single crystal substrates were placed. The block was heated by a built-in resistive tungsten heater, and its temperature was controlled by three chromel-alumel thermocouples. The carbon evaporator was located at the centre of the heating block at a great distance from it. At the same time, the tin evaporator was installed asymmetrically (under one of the corners of the heating block). It means that substrates were located at different distances from the tin evaporator and practically at the same distance from the carbon evaporator. This geometry of the experiment made it possible to obtain a set of samples with different mass thickness of tin on amorphous carbon films of approximately the same thickness.

The thicknesses of condensed layers were estimated by frequency deviation of the quartz resonator in compliance with the geometrical arrangement of evaporators and substrate. To specify the mass thickness of the tin film, the results of the analysis of size island distributions were used.

Two series of samples were prepared. In the first of them, after the condensation (performed on a substrate at room temperature) was completed, the films were heated to temperature of 250°C, which provides the melting of the tin. At this temperature, the samples were within for 5 minutes. The samples of the second series were formed by the vapour-liquid mechanism, *i.e.*, immediately precipitated on a substrate at a temperature of 250°C. After the conclusion of the experiment, the films were cooled to room temperature, then taken from the vacuum chamber and examined in a raster scanning electron microscope Tescan Vega 3 LMH. To provide an effective charge drain, the films were covered with a layer of chromium. The analysis of the obtained images was carried out with to use of original programming software.

In the process of electron-microscopic studies, both images of the plane of the substrate and in its cross sections (cleavages) were taken. The first ones were used to build histograms of the size island distribution, and the second part of them was used to determine the contact angle θ. For measuring θ, the cleavage method was used [23], which consists briefly in the following. The crystal with the film was split in a direction, which was perpendicular to surface of the sample. Further, its edge was examined with the help of electron microscope. The obtained photographs show the profile of drops, which were formed during the melting process (Fig. 1). Up to sizes about 100 μm, the gravity force influence is negligible and drops on unwettable substrate as a result of the action of surface forces have the form of a spherical segment. Such a shape is preserved to a high precision even during crystallization [23]. The drop profile research allows independently determining the geometric parameters of a spherical segment: the radius of curvature of the free surface of the drop R, the diameter of its base

$d = 2r$, and the height H. Any pair of these values determines the contact angle of wetting in accordance with the following relationships:

$$\theta_1 = 2\,\mathrm{arctg}\,\frac{2H}{d}, \quad \theta_2 = \arccos\left(1 - \frac{H}{R}\right),$$
$$\theta_3 = \begin{cases} \arcsin\dfrac{d}{2R}, & \theta < 90°, \\ 180° - \arcsin\dfrac{d}{2R}, & \theta > 90°. \end{cases} \tag{1}$$

In practice, the values of θ_1, θ_2 and θ_3 are somewhat different and therefore an average value was used to improve the accuracy of the angle determination. The spread in values θ_1, θ_2 and θ_3 around the average value is usually 2–3° and characterizes the accuracy of the measurements.

3. RESULTS AND DISCUSSION

According to electron microscopy studies, like for other similar systems [20–22], the samples after the melting process consist of particles of spherical form. Their size depends on the mass thickness of the tin film. The micrographs of island structures obtained as a result of the melting of tin films of different thickness on a carbon substrate are shown in Fig. 2.

Figure 3 shows the dependence of the coverage of substrate by the film (k) on its thickness, which was built for the samples that were subjected to the melting process. For the decaying film, a respectively small coverage of the substrate is typical. It is practically constant in the wide range of thicknesses. Thus, for films, that have the thickness

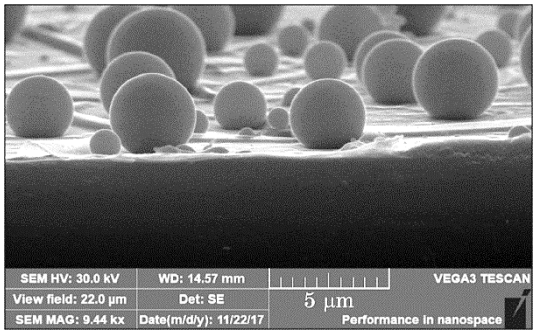

Fig. 1. SEM image of the Sn/C/KCl sample, illustrating the measurement of the contact angles by the cleavage method.

more than 500 nm, k is 0.13–0.15 and very slightly increases with thickness. However, with a decrease of thickness, quite a rapid increase in the growth of the coverage is observed.

To analyse the obtained results, it is necessary for us to consider the energy balance of the process of partitioning plane-parallel film into separate islands. A liquid continuous film on unwettable substrate is unstable and it is energetically advantageous for it to form a structure with a smaller surface.

Let us consider a section of a liquid plane-parallel film with thickness t and area S, which gathers into a single island of equilibrium shape. Such shape will have a drop in the form of a spherical segment with a curvature radius of the surface R by a contact angle θ. A diagram showing the initial and final state of the melting film is shown in Fig. 4.

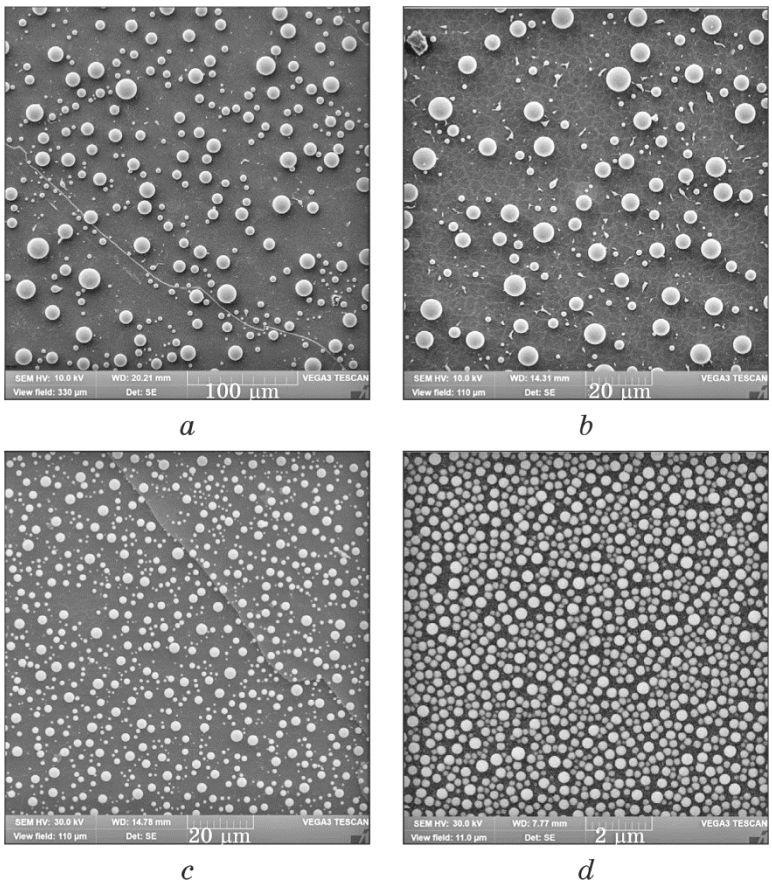

Fig. 2. SEM images of Sn/C films after the melting. The mass thickness of the tin layer: *a*—1000 nm, *b*—420 nm, *c*—275 nm, *d*—70 nm.

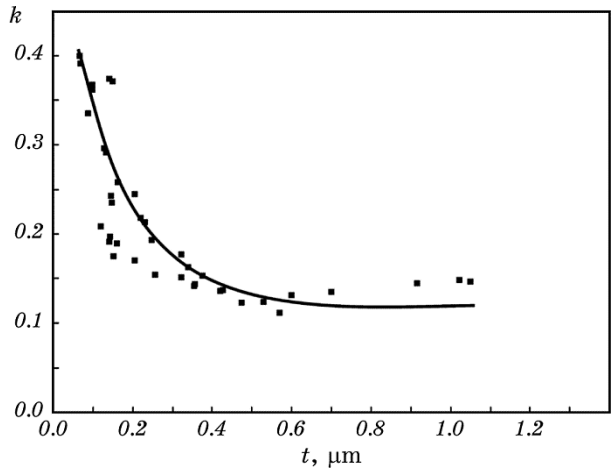

Fig. 3. Dependence of the coverage from the thickness for molten Sn/C films.

The value of the contact angle θ depends on the degree of interaction of the fusion with the substrate and represents itself an individual characteristic of this contact pair. For big drops ($R > 50$ nm), the contact angle does not depend on the size [23]. The droplet radius can be determined from the condition of volume conservation:

$$tS = \frac{4}{3}\pi R^3 \Phi(\theta), \tag{2}$$

where $\Phi(\theta)$ is a geometrical factor that determines the volume of the spherical segment with the angle θ at the base.

The surface energy of a given section of the original film is the next:

$$E_0 = S\sigma_l + S\sigma_{lu}, \tag{3}$$

where σ_l is the surface energy of the free surface of the film (in this case, the liquid fusion) and σ_{lu} is the interfacial energy of the film–substrate interface.

When an island is formed, the area of the free liquid and interfacial

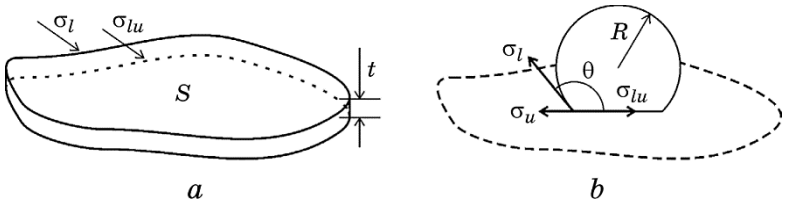

Fig. 4. The shape changing of a film part during the melting process.

surface changes as well as a part of the substrate surface gets free. The surface energy of the final state of the considered section can be written in the following way:

$$E = S_l\sigma_l + S_{lu}\sigma_{lu} + (S - S_{lu})\sigma_u, \tag{4}$$

where S_l is the area of the free surface of a drop, and S_{lu} is the area of the interfacial surface of a drop-substrate

$$S_l = 2\pi R^2(1 - \cos\theta), \quad S_{lu} = \pi R^2 \sin^2\theta. \tag{5}$$

The energy gain (normalized per unit area) due to island's formation is follows:

$$f = \frac{E_0 - E}{S} = \sigma_l + \sigma_{lu} - \sigma_u - \frac{S_{lu}}{S}(\sigma_{lu} - \sigma_u) - \frac{S_l}{S}\sigma_l. \tag{6}$$

Taking into account Young's formula $\cos\theta = (\sigma_u - \sigma_{lu})/\sigma_l$ and the expressions for surface areas bounding a drop (5), a relation (6) can be transformed to following form:

$$f = \sigma_l\left[1 - \cos\theta + \eta\left(\frac{2}{1 + \cos\theta}\right)\right], \tag{7}$$

where $\eta = S_{lu}/S$ is the relative fraction of the interfacial surface. In real conditions, the film is divided into parts of different areas. Respectively, after the melting process, it will consist of particles of different sizes, which represent themselves the similar spherical segments with the same contact angle. The value of η in the case of wetting ($\theta < 90°$) is equal to filling coefficient k, and for $\theta > 90°$ is connected with it by an obvious relation $\eta = k\sin^2\theta$.

It should be noted, that an expression, which is analogical to (7), was obtained in [24] for describing the process of thermal dispersion of a film that occurs without its melting, *i.e.*, in the solid phase. The value of f in this case was interpreted as an additional energy of the polycrystalline film, which is concentrated in the structural imperfections, in particular, in grain boundaries.

In the given research, the film dewetting occurs in the result of its melting, wherein, obviously, all the defects of the crystal structure, including the grain boundaries, disappear. However, the presence of a defective polycrystalline structure in as-deposited films should lead to appearance of an inner size effect [21, 22], which consists in a local decrease of the melting temperature. In addition, the non-equilibrium nature of condensates should affect the particularities of their solid-phase decomposition [20], which is unavoidable as the result of the heating process to pre-melting temperatures. Thus, in spite of the fact

that the dispersion of the films under study is carried out mainly after their melting, the presence of various defects in the initial continuous film has a certain effect on its liquid-phase decomposition.

During the decomposition process into separate islands of already liquid film, the value of f shows the energy gain in this process and characterizes its efficiency in a certain sense. Further, as in the works [25, 26] for f, we will use the term 'excess energy'. The limit value f_∞ corresponds to situation when a film from an infinite area will be gathered into the one drop and determines as asymptote $f_\infty = \sigma_l + \sigma_{lu} - \sigma_u = \sigma_l(1 - \cos\theta)$. This state is unobtainable in view of kinetic factors. However, the approach to this limit indicates the existence of effective mechanisms for mass transferring.

Probably, the predominant mechanism of this process is the liquid flow. At the same time, a liquid-phase mass transfer, carried out on unwettable substrate, is practically unavailable to provide the merge of previously formed disparate drops. Therefore, it can be expected, that for thicker films, which keep entirety to higher temperatures, such a process will be more effective. At the same time, for thin films that segregate into separate islands diffusively even before melting [17], a liquid-phase mass transfer will not have the decisive importance.

An equation (7) in the case of unwetting can be represented in a simpler form:

$$f = \sigma_l(1 - \cos\theta - 4k\Phi(\theta)). \tag{8}$$

The average value of the contact angle in the studied films, which was obtained as a result of the measurements of a large number of particles of different sizes, was 135°. This indicates a poor wetting in the examined contact pair and allows us to conclude, that films under study were in a state close to free.

The size dependence of the excess energy, which is obtained in virtue of the expression (7), is shown in Fig. 5.

As one can see, in a considerable interval of thicknesses, the excess energy f retains practically a constant value. With a decrease in the mass thickness of the film, starting at about 300 nm, a decrease of f is observed up to 0. This means a change in the mechanism of the film's decomposition. For the thinnest samples, even a sign change occurs, which is physically impossible within the framework of the model under consideration. An obvious explanation of this phenomenon lies in the fact that films of such thicknesses break up into separate islands long before melting or even take the form of islands immediately after the deposition. This was successfully proved by SEM studies. Therefore, another value of E_0 is peculiar to such films and application of the relation (7) to them is irregular. The non-continuity of the film in the

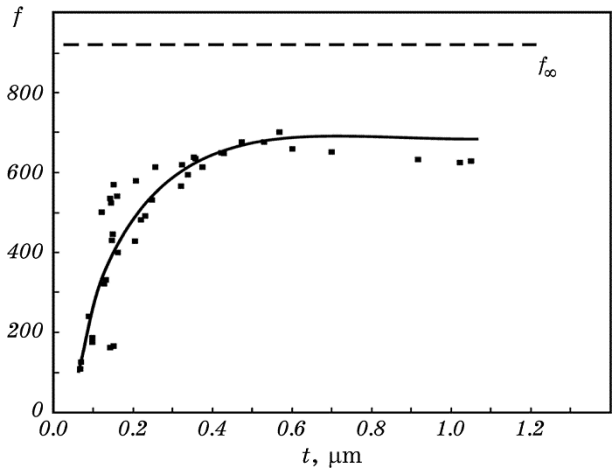

Fig. 5. Dependence of the excess energy of Sn/C films on the mass thickness of the tin film; dashed line corresponds to limit value of the excess energy f_∞.

initial state or that one, which appeared during the heating even before melting, is the reason of the depression of f with decreasing of the mass thickness.

Along with sufficiently thin molten films, the high factors of coverage are peculiar to Sn/C films, which were obtained due to condensation mechanism of liquid vapour (Fig. 6). For such samples, regardless of their thickness, the use of the formula (9) leads to a negative value of the excess energy. In contrast to the films, which are condensed in a solid phase, such samples are already of island structure as a result of

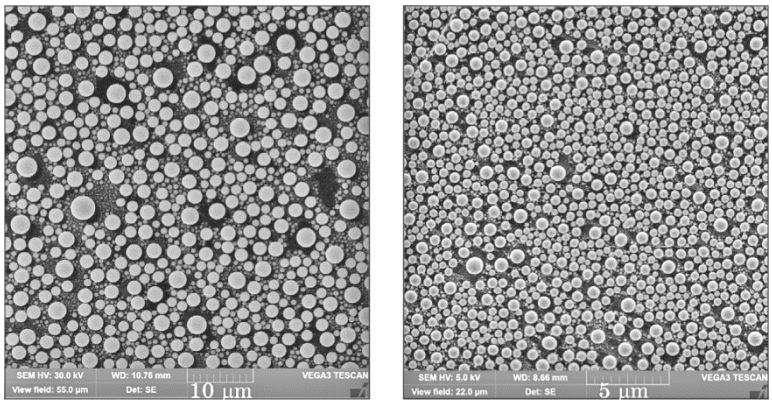

a *b*

Fig. 6. SEM images of Sn/C films obtained as a result of tin condensation into liquid phase.

the preparation process. This leads to the fact, that they do not contain defects, which are typical for polycrystalline films and, therefore, are placed closer to equilibrium state. In addition, the mechanisms of liquid-phase mass transfer, which provide the formation of large particles during the decomposition of continuous films, are ineffective for island structures.

At the same time, as it follows from the results of the Refs. [17, 21, 27], the intensity of the continuous film decomposition into individual islands increases with the decrease of its thickness. Thus, a rapid increase in the filling coefficient for sufficiently thin samples can be explained by the fact, that the films with the thickness of more than 400 nm preserve the continuity practically up to melting temperature, at which their decomposition is carried out in the way of the liquid-phase mass transfer. At the same time, the thinner samples to the moment of the formation of the liquid phase already have managed to break into separate islands, which are freer from the excess stresses in comparison with solid films. Gradually, with an increase of the dispersion degree, the proportion of the excess energy, which is contained in the island, decreases, and for films with a thickness of less than 40 nm, each of the islands of the crystalline film generates, probably, a separate spherical particle.

The planar images, which are presented in Fig. 2, allowed us to construct the histograms of particle size distribution (Fig. 7). Such histo-

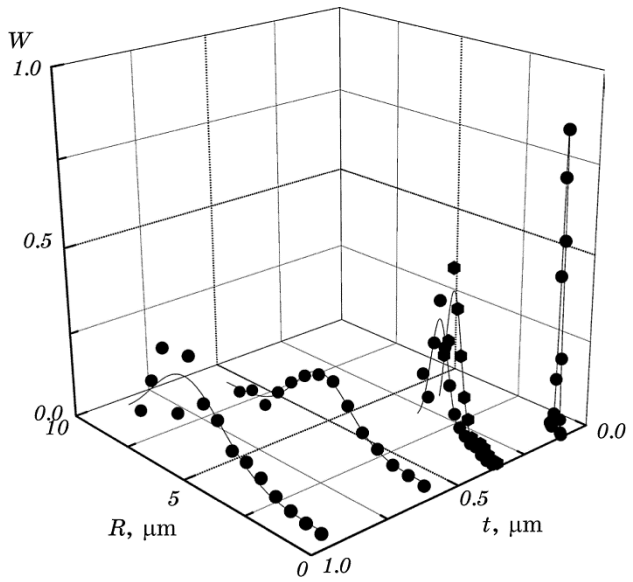

Fig. 7. Histograms of particle size distribution in Sn/C films after the melting process.

grams are of great importance for the technological aspects of using the formed disperse systems. In Figure 7 the value of W, determined on the vertical axis, is defined by the following relation

$$W = \frac{4}{3}\frac{\pi N(R)R^3}{A\Delta R},$$

where $N(R)$ is the number of particles, the radius of which falls into selected step of constructing the histogram ΔR, A is the area of the image, from which the histogram calculation was carried out. The choice of such histogram normalization [28] allows us to display the islands distribution by the volume, which, actually, makes sense for different technological applications.

It can be seen from the Fig. 7, that the particle size distributions on which the films of the studied thicknesses decay, contain one maximum. The thinner films are characterized by narrow diagram with a maximum in small-size region. With an increase in the thickness of the original film, the width of the distributions increases and their maximum is shifted to the region of bigger sizes. The results of a quantitative analysis of the distributions are shown in Fig. 8. For their construction, the experimental data (Fig. 7) were approximated by the Gaussian distribution, from which the half-width of the curves and their maximum, *i.e.*, the most probable radius of particles in the films after their dispersion, were determined. It can be seen, that both values increase practically linearly with the thickness of the original film.

Note the fact, that expression (8) does not contain in an explicit form the dependence on t, and in a wide interval of mass thicknesses such dependence is not really observed experimentally. On the hy-

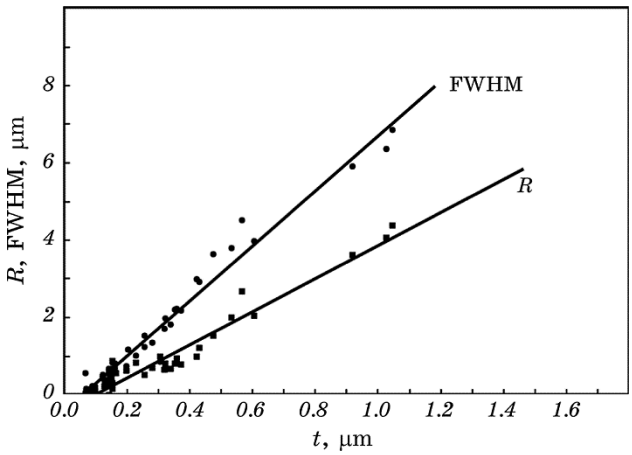

Fig. 8. Dependence of the most probable radius (R) and half-width of the histogram of the volume distribution on the Sn/C film thickness (t).

pothesis that the film is divided into drops of the same size, the expression (8) can be written not by the formula of the coverage, but by t and R, using the explicit expressions for the drop volume (2) and the area of its base (5)

$$f = \sigma_l(1 - \cos\theta - 3t/R), \tag{9}$$

The dependence of the excess energy on the thickness of the original film, which was obtained in this way, is shown in Fig. 9. Its character repeats a similar dependence in whole, which is based by reference to the data about the dependence of the coverage factor on t.

It should be noted, that narrowing of histograms during decreasing of the film thickness has a great technological importance. After the melting process of enough thin films, the arrays of practically spherical particles are formed, which have quite a narrow histogram of distribution and a large coverage factor. Such objects look attractive from viewpoint of the possibility of the application using. At the same time, the problem of controlling the particle size distribution is no less important. The break of the coverage factor dependences and excess energy on the mass thickness seems to be correspondent to the change in the film dispersion mechanism.

At small thicknesses the film decay into the islands occurs diffusively in the solid phase, but at large thicknesses, it occurs after the melting process in the form of a liquid-phase flow. The relaxation processes, which occur in the solid phase, are normally accompanied by a decrease in the proportion of the excess energy in the previously dis-

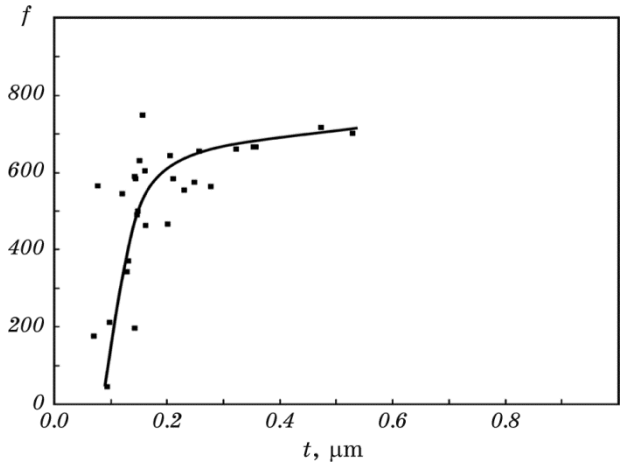

Fig. 9. Dependence of the excess energy on thickness of continuous films, which was obtained from the data of the size dependence of the most probable particle's radius formed during the melting process.

persed structure, which allows us to indicate a direction of possible control of the histogram's parameters. By virtue of the fact that narrower distributions are typical for films with a smaller fraction of the excess energy, it can be assumed, that the preliminary annealing, during which the films in one or another way get rid of available mechanical stresses, should provide narrower distributions for the particles, which are formed during the following melting process of the film.

4. CONCLUSION

The study of the structures formed during the melting process of initially continuous Sn/C films was carried out. It was shown, that the most probable radius of the particles, which were formed during the melting process of the films and the half-width of the corresponding histograms increase practically linearly with the film thickness. Moreover, it was determined that the substrate coverage factor with a film in the samples, which were subjected to melting process, with a thickness of the original film of more than 300 nm, has a practically constant value and is about 15%. At the same time, in thinner films, the filling coefficient sharply increases and in samples, which initial thickness is less than 150 nm, it tends to values, which are typical for the films formed by the vapour-liquid mechanism. A size dependence of the excess energy was obtained. As shown, it decreases fast for the films with a thickness of less than 300 nm. This means that the dispersion of such films and the corresponding relaxation of the stresses, existing in them, occur even in the solid phase, *i.e.*, before the melting process.

REFERENCES

1. H. Lauter, V. Lauter-Pasyuk, B.Toperverg, L. Romashev, M. Milyaev, T. Krinitsina, E. Kravtsov, V. Ustinov, A. Petrenko, and V. Aksenov, *J. Magn. Magn. Mater.*, **258–259**: 338 (2003).
2. Yu. N. Khaydukov, A. S. Vasenko, E. A. Kravtsov, V. V. Progliado, V. D. Zhaketov, A. Csik, Yu. V. Nikitenko, A. V. Petrenko, T. Keller, A. A. Golubov, M. Yu. Kupriyanov, V. V. Ustinov, V. L. Aksenov, and B. Keimer, *Phys. Rev. B*, **97**: 144511 (2018).
3. A. B. Drovosekov, N. M. Kreines, A. O. Savitsky, E. A. Kravtsov, D. V. Blagodatkov, M. V. Ryabukhina, M. A. Milyaev, V. V. Ustinov, E. M. Pashaev, I. A. Subbotin, and G. V. Prutskov, *J. Exper. Theor. Phys.*, **120**, No. 6: 1041 (2015).
4. Himanshu Gupta, Fateh Singh Gill, S. K. Sharma, R. Kumar, and R. M. Mehra, *J. Nano- Electron. Phys.*, **10**, No. 3: 03014 (2018).
5. Rupali Kulkarni, Amit Pawbake, Ravindra Waykar, Ashok Jadhawar, Haribhau Borate, Rahul Aher, Ajinkya Bhorde, Shruthi Nair, Priyanka

Sharma, and Sandesh Jadkar, *J. Nano- Electron. Phys.*, **10**, No. 3: 03005 (2018).
6. R. N. Zhukov, T. S. Ilina, E. A. Skryleva, B. R. Senatulin, I. V. Kubasov, D. A. Kiselev, G. Suchaneck, M. D. Malinkovich, Yu. N. Parkhomenko, and A. G. Savchenko, *J. Nano- Electron. Phys.*, **10**, No. 2: 02009 (2018).
7. H. H. Jeong, A. G. Mark, M. Alarcyn-Correa, I. Kim, P. Oswald, T. C. Lee, and P. Fischer, *Nature Commun.*, **7**: 11331 (2016).
8. J. Chen, H. Che, K. Huang, C. Liu, and W. Shi, *Appl. Catalysis B: Environmental*, **192**: 134 (2016).
9. J. Gan, B. B. Rajeeva, Z. Wu, D. Penley, C. Liang, Y. Tong, and Y. Zheng, *Nanotechnology*, **27**, No. 23: 235401 (2016).
10. T. I. Borodinova, V. I. Styopkin, A. A. Vasko, V. Ye. Kutsenko, and O. A. Marchenko, *J. Nano- Electron. Phys.*, **10**, No. 3: 03017 (2018).
11. B. I. Turko, V. B. Kapustianyk, L. R. Toporovska, V. P. Rudyk, V. S. Tsybulskyi, and R. Y. Serkiz, *J. Nano- Electron. Phys.*, **10**, No. 2: 02002 (2018).
12. S. Wahyuningsih, F. N. Ainiy, and A. H. Ramelan, *J. Nano- Electron. Phys.*, **10**, No. 1: 01004 (2018).
13. P. A. Kumar, S. Mitra, and K. Mandal, *Indian J. Pure Appl. Phys.*, **45**, No. 1: 21 (2007).
14. S. B. Dalavi and R. N. Panda, *J. Magn. Magn. Mater.*, **374**, No. 15: 411 (2015).
15. V. O. Yukhymchuk, O. M. Hreshchuk, M. Y. Valakh, M. A. Skoryk, V. S. Efanov, and N. A. Matveevskaya, *Semicond. Phys. Quantum Electron. Optoelectron.*, **17**, No. 3: 217 (2014).
16. Yu. V. Naidich, I. I. Gab, T. V. Stetsyuk, B. D. Kostyuk, and S. I. Martynuyk, *Metallofiz. Noveishie Tekhnol.*, **37**, No. 9: 1225 (2015) (in Ukrainian).
17. S. I. Petrushenko, S. V. Dukarov, and V. N. Sukhov, *Metallofiz. Noveishie Tekhnol.*, **38**, No. 10: 1351 (2016) (in Ukrainian).
18. S. I. Petrushenko, S. V. Dukarov, and V. N. Sukhov, *Vacuum*, **142**: 29 (2017).
19. S. V. Dukarov, S. I. Petrushenko, V. N. Sukhov, and I. G. Churilov, *Problems Atomic Sci. Technol.*, **89**, No. 1: 110 (2014).
20. A. P. Kryshtal, *Appl. Surf. Sci.*, **321**: 548 (2014).
21. S. I. Petrushenko, S. V. Dukarov, V. N. Sukhov, and I. G. Churilov, *J. Nano- Electron. Phys.*, **7**, No. 2: 2033-1 (2015).
22. S. V. Dukarov, S. I. Petrushenko, V. N. Sukhov, I. G. Churilov, A. L. Samsonik, and O. I. Skryl, *Acta Phys. Polonica A*, **133**, No. 5: 1186 (2018).
23. N. T. Gladkikh, S. V. Dukarov, A. P. Krishtal', V. I. Larin, V. N. Sukhov, and S. I. Bogatyrenko, *Poverkhnostnye Yavleniya i Fazovye Prevrashcheniya v Kondensirovannykh Plenkakh* [Surface Phenomena and Phase Transformations in Condensed Films] (Kharkiv: KHNU imeni V. N. Karazina: 2004) (in Russian).
24. P. G. Vassilev, *Bulgarian J. Phys.*, **3**: 184 (1976).
25. A. P. Kryshtal, *Appl. Surf. Sci.*, **321**: 548 (2014).
26. A. P. Kryshtal, N. T. Gladkikh, and R. V. Sukhov, *Appl. Surf. Sci.*, **257**, No. 17: 7649 (2011).
27. A. A. Minenkov, S. I. Bogatyrenko, R. V. Sukhov, and A.P. Kryshtal, *Phys. Solid State*, **56**, No. 4: 823 (2014).
28. S. V. Dukarov, S. I. Petrushenko, and V. N. Sukhov, *J. Nano- Electron. Phys.*, **10**, No. 1: 01023 (2018) (in Russian).